Bioconjugate Chemistry

Article

pubs.acs.org/bc

# Tumor-Targeting Transferrin Nanoparticles for Systemic Polymerized siRNA Delivery in Tumor-Bearing Mice

Ji Young Yhee,[†,⊥] So Jin Lee,[†,⊥] Sangmin Lee,[†,‡] Seungyong Song,[†,‡] Hyun Su Min,[†] Sun-Woong Kang,[§] Sejin Son,[†] Seo Young Jeong,[‡] Ick Chan Kwon,[†,∥] Sun Hwa Kim,*[,†] and Kwangmeyung Kim*[,†]

[†]Center for Theragnosis, Korea Institute of Science and Technology, 39-1 Hawolgok-dong, Sungbuk-gu, Seoul 136-791, South Korea

[‡]Department of Life and Nanopharmaceutical Sciences, Kyung Hee University, 1 Hoegi-dong, Dongdaemun-gu, Seoul 130-701, South Korea

[§]Next-generation Pharmaceutical Research Center, Korea Institute of Toxicology, Daejeon 305-343, South Korea

[∥]KU-KIST School, Korea University, 1 Anam-dong, Seongbuk-gu, Seoul 136-701, South Korea

*S* *Supporting Information*

**ABSTRACT:** Transferrin (TF) is widely used as a tumor-targeting ligand for the delivery of anticancer drugs because the TF receptor is overexpressed on the surface of various fast-growing cancer cells. In this article, we report on TF nanoparticles as an siRNA delivery carrier for in vivo tumor-specific gene silencing. To produce siRNA carrying TF nanoparticles (NPs), both TF and siRNA were chemically modified with sulfhydryl groups that can build up self-cross-linked siRNA-TF NPs. Self-polymerized 5′-end thiol-modified siRNA (poly siRNA, psi) and thiolated transferrin (tTF) were spontaneously cross-linked to form stable NPs (psi-tTF NPs) under optimized conditions, and they could be reversibly degraded to release functional monomeric siRNA molecules under reductive conditions. Receptor-mediated endocytosis of TF induced rapid tumor-cell-specific uptake of the psi-tTF NPs, and the internalized NPs resulted in a downregulation of the target protein in red-fluorescent-protein-expressing melanoma cancer cells (RFP/B16F10) with negligible cytotoxicity. After systemic administration, the psi-tTF NPs showed marked accumulation at the tumor, leading to successful target-gene silencing in vivo. This psi-tTF NP system provided a safe and effective strategy for in vivo systemic siRNA delivery for cancer therapy.

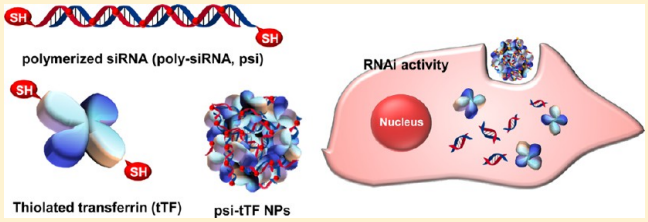


## ■ INTRODUCTION

RNA interference (RNAi) is induced by 21 to 25 nucleotides of small interfering RNA (siRNA), which participates in target-gene silencing by binding the RNA-induced silencing complex to degrade complementary mRNA molecules.[1−3] During the past decade, siRNA has attracted considerable attention as a potential therapeutic agent and as a potent therapeutic strategy for incurable diseases because of its high specificity in targeted gene silencing.[2−4] The technique of siRNA-mediated gene silencing offers a feasible strategy for cancer treatment because the overexpression of a variety of oncogenes is often closely related with tumorigenesis and cancer progression.[2,4] However, clinical use of siRNA for therapeutic purposes is still limited because of problems with siRNA delivery as a result of the instability and poor cellular uptake of siRNA.

To overcome these limitations, a variety of viral and nonviral vector systems have been engineered for effective siRNA delivery. Viral vectors generally demonstrate a higher transfection efficiency, but current RNAi research studies are mainly focused on nonviral vectors because of their low cost, safety, and ease of manufacturing.[5−7] Cationic polymer-based vehicles have been the most commonly used because of their strong electrostatic affinity to nucleic acids, leading to the formation of condensed nanosized complexes.[8,9] Unfortunately, cationic polymers show low transfection efficiency and have considerable toxicity, limiting their clinical use.[6,10] Furthermore, cationic polymer-based vehicles are more severely restricted by low target specificity, especially when administered systemically.

An ideal siRNA delivery system for cancer therapy should satisfy both safety and selectivity criteria. From this perspective, transferrin (TF), a serum protein, is a good candidate for an siRNA carrier because of its biocompatibility and tumor-targeting ability. Transferrin has been widely used as a cancer-targeting agent because proliferating and malignant cancer cells usually overexpress transferrin receptors on their cell surface.[11,12] In practice, several transferrin conjugates as drug carriers demonstrated prolonged circulation in the blood and a high affinity for cancer cells because of the TF receptor-mediated endocytosis mechanism.[13−16] However, natural TF does not possess sufficient binding affinity for negatively charged nucleic acids and thus cannot be utilized as a gene carrier.

The purpose of this study was to investigate the utility of TF as a biocompatible and tumor-targetable siRNA carrier for use

**Received:** May 6, 2013
**Revised:** September 21, 2013
**Published:** October 9, 2013

in systemic administration in cancer therapy. To improve the binding affinity between TF and siRNA, both molecules were chemically modified with sulfhydryl groups. The resulting thiolated TF (tTF) built self-cross-linked transferrin nanoparticles (NPs), and self-polymerized 5′-end thiol-modified siRNA (poly siRNA) was encapsulated in the NPs. Consequently, the encapsulated siRNA molecules were protected from degradation by nucleases in the serum and delivered to the cytoplasm of the cancer cells by receptor-mediated endocytosis. Moreover, the siRNA-carrying tTF NPs (psi-tTF NPs) showed an extended circulation time in the blood and a marked accumulation at the tumor site in vivo. The results may provide useful tools for expanding the potential applications of TF for cancer therapy using siRNA.

## EXPERIMENTAL PROCEDURES

**Materials.** Human holo-transferrin was used in this study because TF receptor proteins from mouse and human have significant similarity, exhibiting about 90% identity at the amino acid level.[17,18] TF (holo-transferrin ≥98%, $M_w$ = 75 kDa), 2-iminothiolane HCl, *N*-(2-hydroxyethyl) piperazine-*N*′-ethanesulfonic acid (HEPES), ethylenediaminetetraacetic acid (EDTA), 1,4-dithiothreitol (DTT), fluorescein isothiocyanate (FITC) isomer, and ethidium bromide (EtBr) were purchased from Sigma (St. Louis, MO, USA). Near-infrared fluorescence (NIRF) dye Flamma (FPR-675) was obtained from Bioacts (Seoul, Korea). RFP-targeted siRNA for visualizing gene suppression as well as the scrambled sequence of siRNA was synthesized and annealed at Bioneer (Seoul, Korea). The sequence of the RFP-targeted sense strand is 5′-UGU AGA UGG ACU UGA ACU CdTdT-3′, and the antisense strand sequence is 5′-GAG UUC AAG UCC AUC UAC AdTdT-3′. The sequence of the scrambled sense strand is 5′-UGA AGU UGC ACU UGA AGU CdTdT-3′, and the antisense strand sequence is 5′-GAC UUC AAG UGC AAC UUC AdTdT-3′.[19,20] Cell culture reagents and RNase-free distilled water were from Invitrogen (Carlsbad, CA, USA), and all of the solutions were prepared in RNase-free distilled water and autoclaved prior to use.

**Preparation of Poly siRNA, Thiol-Modified TF, and psi-tTF NPs.** The 5′ end of each sense and antisense strand of siRNA (1 mg, 0.076 μmol) was thiol-modified to enable it to be self-polymerized.[21] Dithiol-modified siRNA molecules in DEPC-treated ultrapure water were incubated with DTT (5 mM) for 1 h to expose the functional thiol groups. Then, they were purified using a Nap-10 desalting column (GE Healthcare) for lyophilization. The lyophilized siRNA molecules were self-polymerized in HEPES buffer (10 mM, pH 8.0) under mild oxidative conditions. The conformation and reducibility of poly siRNA were visualized on an 8% polyacrylamide gel. The reducibility of the poly siRNA was investigated using gel electrophoresis with 1 μg of poly siRNA after DTT treatment (10 mM, 3 h).

TF was functionalized by introducing the thiol groups to prepare self-cross-linked TF NPs to encapsulate poly siRNA. TF was thiolated using 2-iminothiolanes under oxygen-limiting conditions, and the extent of the thiolation was determined by Ellmann's assay.[22] A total of 10 mg of TF and 1 mg of 2-iminothiolane HCl (1:50 mol ratio) was dissolved in 1 mL and 100 μL of 0.1 M sodium phosphate EDTA buffer (pH 8.0, PB buffer), respectively. The mixing solution was then reacted at 4 °C for 1 h. The solution was dialyzed for 7 h at 4 °C in distilled water (molecular weight cut off = 3 kDa) and lyophilized prior to use. To optimize the mixing ratio (psi/tTF) of the psi-tTF NPs, the lyophilized tTF was dissolved in RNase-free PB buffer (pH 8.0, 10 μg/μL) and immediately mixed with poly siRNA in RNase-free HEPES buffer (pH 8.0, 1 μg/μL) at a weight ratio ranging from 1:5 to 1:20. Each mixture solution in the test tube was sealed and incubated at 37 °C. To optimize the incubation time, gel retardation and size distribution were time-dependently monitored. The complex formation was confirmed using a gel-retardation assay and transmission electron microscopy (TEM) imaging (CM 200 electron microscope, Philips). Under the optimized conditions, unthiolated TF and monomeric siRNA (mono-siRNA) were also tested to identify their binding potential and their affinity for forming complexes.

**Characteristics of the psi-tTF NPs.** To measure the size and the zeta potential of the particles, dynamic light scattering (DLS; Spectra Physics Laser, Model 127-35, Mountain View, CA, USA) and an electrophoretic light-scattering spectrometer (Ostuka, Electronics Co., Ltd., Japan) were used. The morphology of the NPs was observed by TEM. To visualize the stability of the psi-tTF NPs against RNase degradation, each poly siRNA and psi-tTF, including 1 μg of siRNA, was incubated with 0.3 U of RNase A at 37 °C for 0 to 12 h. After the incubation, disulfide linkages were cleaved by DTT treatment (10 mM), and the remaining RNA molecules of 21 bp were quantitatively compared using gel imaging (MiniBIS Pro, DNR Bio-Imaging Systems, Jerusalem, Israel).

**In Vitro Cellular Uptake of the psi-tTF NPs.** To visualize the cellular uptake of the psi-tTF NPs, FITC-labeled TF and FPR-675-labeled poly siRNA were used for complexation. Cancer cells from squamous cell carcinoma and melanoma that overexpress the TF receptor were used in this study.[23−25] Murine squamous cell carcinoma cells (SCC-7; American Type Culture Collection, Rockville, MD, USA) and melanoma cells (B16F10; donated from Kyungpook University, Korea) ($1 \times 10^5$ cells per 35 mm cover-glass on the bottom of a culture plate) were treated with dual-labeled psi-tTF NPs (100 nM siRNA included) in serum-free opti-MEM media for 5 h. After fixation, the nuclei were stained with diamidino-2-phenylindole (DAPI). The fluorescence microscopic images were acquired using an IX81-ZDC focus drift compensating microscope (Olympus, Tokyo, Japan). We also validated receptor-mediated endocytosis of the psi-tTF NPs through a TF receptor competition-binding assay. In the competition experiments, the cellular uptake of the psi-tTF NPs was investigated in the opti-MEM media supplemented with 100 μg/mL of free TF.

**Cytotoxicity and in Vitro Gene Silencing of the psi-tTF NPs.** The cytotoxicity of the psi-tTF NPs was evaluated using the 3-(4,5-dimethylthiazol-2-yl)-2,5-diphenyltetrazolium bromide (MTT) assay. The SCC-7 cells ($5 \times 10^3$ cells in 96-well plates) were exposed to different concentrations of psi-tTF NPs containing 25−400 nM siRNA at 37 °C for 48 h followed by the addition of 20 μL of MTT solution. Cell viability was determined by measuring the differences in the optical absorbance at 570 nm.

The gene-silencing efficacy of the psi-tTF complexes was visualized with RFP-expressing B16F10 cells (RFP/B16F10) as previously described.[20] The RFP/B16F10 cells ($1 \times 10^5$ cells per 35 mm dish) for psi-tTF NPs treatment were replaced with serum-free opti-MEM media 1 h prior to the transfection, and the cells were exposed to the psi-tTF NPs at a dose of 200 nM siRNA. The RFP poly siRNA formulated in the commercial transfection reagent Lipofectamine (LF; Invitrogen, Carlsbad, CA, USA) was used as a positive control. Opti-MEM media

Scheme 1. Schematic Diagram of (A) Poly siRNA, (B) Thiolated TF, and (C) psi-tTF NPs

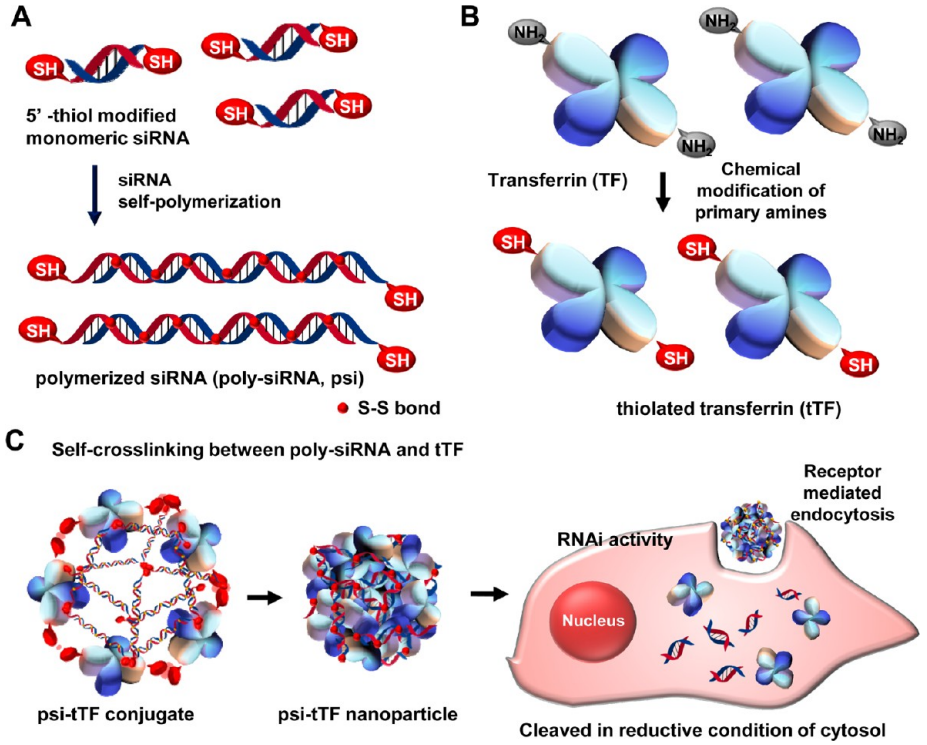


without siRNA complexes and scrambled poly siRNA in tTF NPs (psi(sc)-tTF NPs) were used as negative controls. Each formulation was treated for 5 h, and the media was replaced with fresh RPMI media after the transfection. After 48 h of further incubation, the cells were fixed to observe the RFP signals using fluorescence microscopy at 100× magnification. The number of total cells and RFP-expressing cells were counted in four random fields (400× magnification), and the ratio of the RFP-expressing cells to total cells for the control was defined as 100%.

**Animal Tumor Models.** All of the animal experiments were performed in compliance with the relevant laws and institutional guidelines of the Korea Institute of Science and Technology (KIST). To avoid fluorescence interference by the melanin pigment of the B16F10 cells, we decided to monitor the in vivo real-time psi-tTF complex distribution with only SCC-7 tumor-bearing mice. SCC-7 tumor-bearing mice were prepared by subcutaneous injection of $5 \times 10^5$ SCC-7 cells suspended in 60 $\mu$L of serum-free media into male athymic nude mice ($n$ = 4, Institute of Medical Science, Tokyo). To determine the in vivo gene silencing, RFP/B16F10 tumor-bearing mice ($n$ = 10) were also prepared by subcutaneous inoculation of RFP/B16F10 cells ($5 \times 10^5$ cells in 60 $\mu$L of serum-free media) into the left flank of nude mice.

**In Vivo Distribution of the psi-tTF NPs.** After 14 days from the time of tumor-cell implantation, FPR-675-labeled psi-tTF NPs and naked poly siRNA were intravenously injected into the SCC-7 tumor-bearing mice at a dose of 40 $\mu$g of poly siRNA. Time-dependent whole body NIRF imaging was monitored using the eXplore Optix System (Advanced Research Technologies Inc., Montreal, Canada) for up to 24 h, and the total photon flux in the tumor tissue was quantified using Analysis Workstation software. After the imaging, tumors and major visceral organs were excised from the mice to compare the NIRF intensity using a KODAK imaging station (4000 MM; Kodak, New Haven, CT, USA). The NIRF in the organs was quantified to compare the relative accumulation of siRNA molecules in the tumors.

**Gene Silencing of the psi-tTF Complex in Tumor-Bearing Mice.** When the diameter of the RFP/B16F10 tumors increased to 4 ± 0.5 mm in size, the mice were divided into RFP-matched pairs, with each pair showing an equal amount of RFP expression. In the three RFP-matched pairs, psi or the psi-tTF NPs was injected (40 $\mu$g of poly siRNA/mouse) via the tail vein every 48 h on days 0, 2, and 4. To exclude RFP downregulation by a nonspecific mechanism in vivo, two matched pairs were prepared as nontreated and psi(sc)-tTF NPs treated controls. To evaluate the in vivo gene-silencing efficacy of the psi-tTF NPs, the fluorescence intensity of the RFP tumor was monitored in paired mice using the KODAK imaging station. After 6 days, all of the mice were sacrificed to obtain the tumor tissues to measure the fluorescence intensity. The illumination conditions (lamp voltage, filter set, exposure time, etc.) were identical for each tumor imaged. To assess further the RFP expression in the tumor tissues, the excised tumors were embedded in optimum cutting temperature tissue compound (OCT compound, Sakura, Tokyo) for cryosectioning. Each 8 $\mu$m thick frozen section was stained with DAPI and observed with fluorescence microscopy.

## RESULTS

**Preparation and Physiochemical Properties of psi-tTF NPs.** Scheme 1 shows a schematic representation of the preparation of the psi-tTF NPs. First, we prepared poly siRNA from the self-polymerization of 5′-end thiol-modified siRNA molecules (Scheme 1A).[21] Thiol-modified sense and antisense strands of siRNA molecules were successfully self-polymerized to give a higher molecular weight of poly siRNA. To use the TF-based NPs as poly siRNA carriers, natural TF was also modified with 2-iminothiolane HCl (Scheme 1B). A molecule

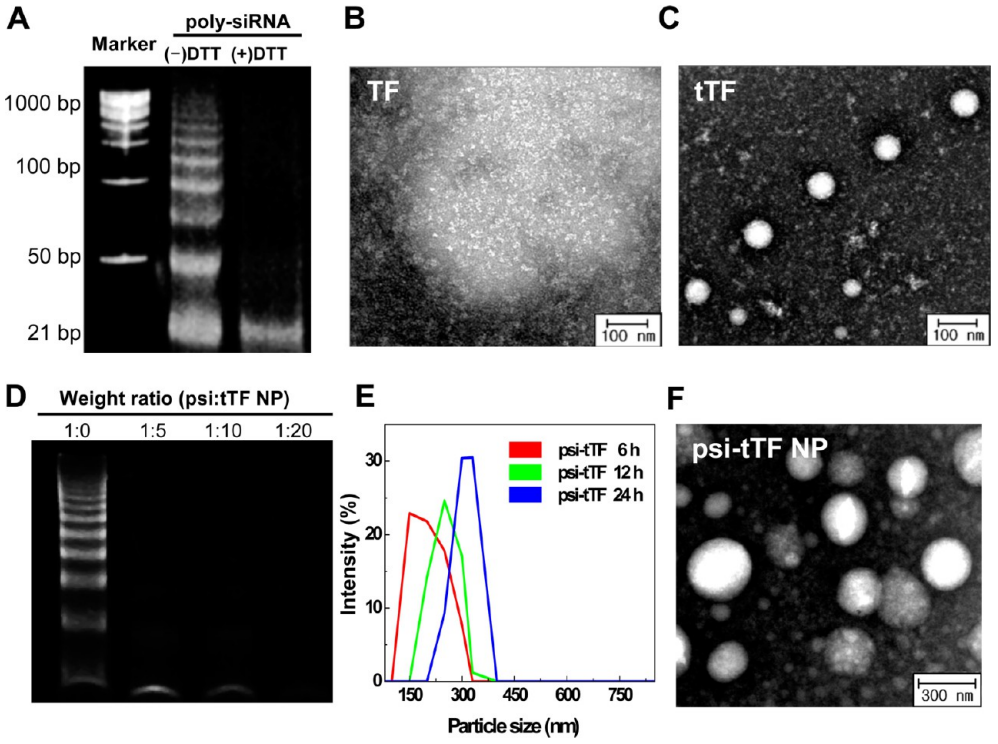


**Figure 1.** Development of psi-tTF NPs and physicochemical characterization. (A) Poly siRNA and a reduction test of poly siRNA by adding DTT. (B) TEM images of natural TF. (C) TEM images of tTF. (D) Gel-retardation assay of complexes of poly siRNA with tTF at different weight ratios (1:5, 1:10, and 1:20). (E) Time-dependent particle-size distribution of the psi-tTF NPs. (F) TEM images of psi-tTF NP.

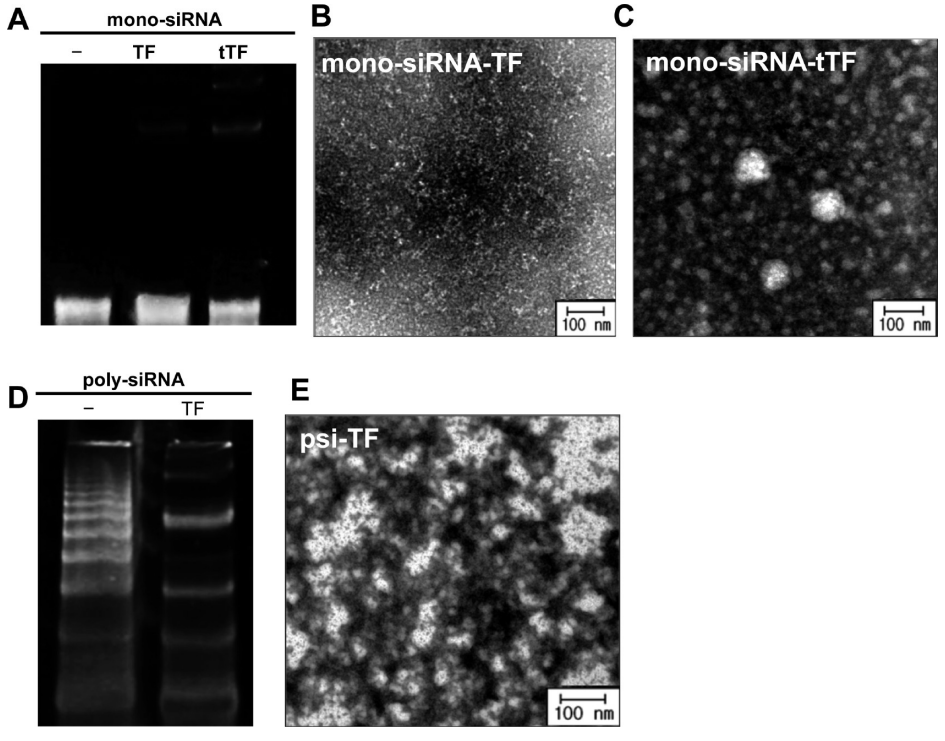


**Figure 2.** Ability to build nanostructures before thiol modification of TF and siRNA. (A) Gel-retardation assay of mono siRNA natural TF and mono siRNA tTF. (B) TEM images of mono siRNA TF. (C) TEM images of mono siRNA tTF. (D) Gel-retardation assay of psi-TF. (E) TEM images of psi-TF.

of unthiolated TF, which consists of a single chain of 679 amino acids including 58 lysine residues, has surface primary amine residues for introducing free sulfhydryl groups. Among the exposed primary amines, 8.7 sulfhydryl groups, on average, were introduced in a TF molecule. During the incubation, poly siRNA and tTF formed psi-tTF conjugates through a chemical cross-linking reaction. Finally, the psi-tTF conjugates spontaneously formed dense and stable NP structures through


dx.doi.org/10.1021/bc400226b | *Bioconjugate Chem.* 2013, 24, 1850−1860

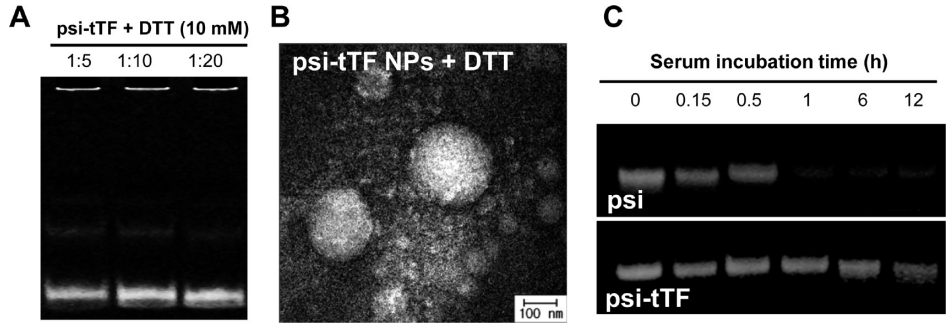


**Figure 3.** Disruption of psi-tTF NPs under reductive conditions and stability of siRNA under RNase A treatment conditions. (A) Gel-retardation assay of psi-tTF NPs after DTT treatment. (B) TEM image of psi-tTF NPs after DTT treatment. (C) Stability of naked poly siRNA and psi-tTF after RNase A treatment.

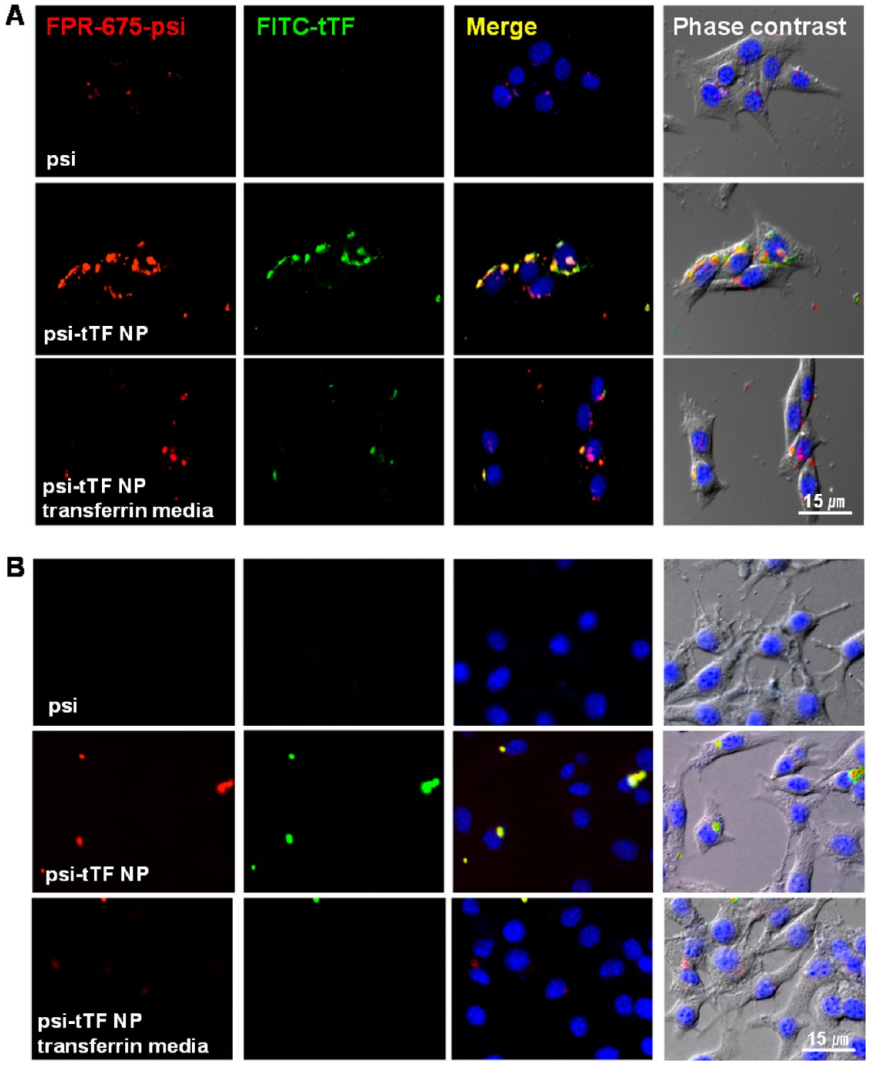


**Figure 4.** In vitro cellular uptake of psi-tTF NPs. Fluorescence images of SCC-7 cells (A) and B16F10 cells (B) treated with naked psi (upper) and psi-tTF NPs in the absence (middle) or presence (lower) of free TF. FITC-labeled tTF and FPR-675-labeled siRNA are shown in green and red, respectively. The merged images are shown in yellow, representing the colocalization of tTF and poly siRNA. The transfections of psi-tTF NPs were carried out at the dose of 30.8 $\mu$g/mL, which included 100 nM siRNA.

intermolecular cross-linking of the tTF molecules, resulting in psi-tTF NPs (Scheme 1C).

The poly siRNA showed a ladderlike migration pattern in 8% polyacrylamide gel electrophoresis (PAGE). The molecular-weight distribution of the poly siRNA was between 21 and 1000 bp. Each band fraction of poly siRNA was quantitatively analyzed, and 68% of poly siRNA molecules, on average, were above 100 bp. On average, poly siRNA showed 6 times more anionic charges per molecule compared to mono siRNA. The poly siRNA was reversibly degraded into mono-siRNA molecules under reductive conditions (Figure 1A), suggesting that the poly siRNA could be uncondensed to release


dx.doi.org/10.1021/bc400226b | *Bioconjugate Chem.* 2013, 24, 1850−1860

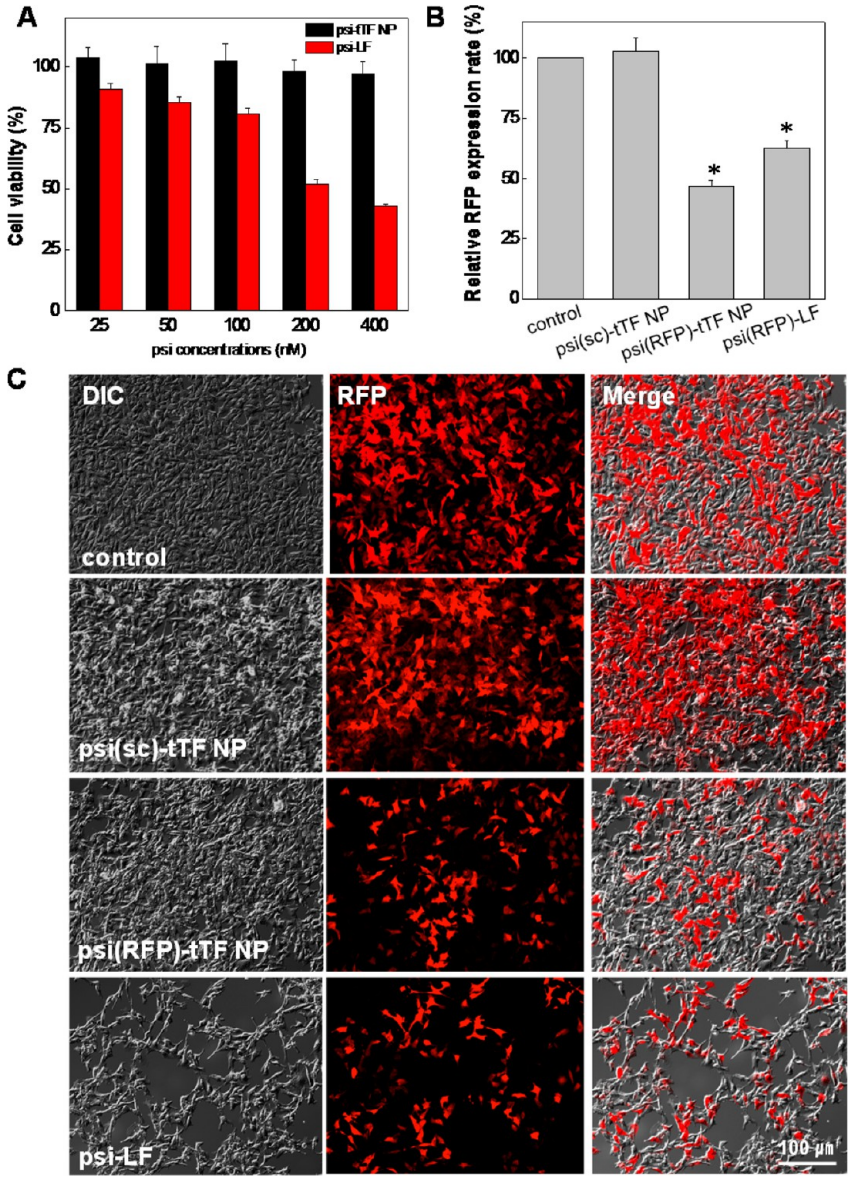


**Figure 5.** Cytotoxicity and in vitro gene-silencing efficacy of psi-tTF NPs in RFP-expressing B16F10 cells. (A) Cytotoxicity of psi-tTF and psi-LF complexes at various concentrations of siRNA formulation from 25 to 400 nM. (B) Relative RFP-expression rate after the transfection using psi-tTF and psi-LF (200 nM siRNA). * $p < 0.05$ compared to control. (C) Fluorescence microscopic images of RFP/B16F10 cells after transfection using psi(sc)-tTF NPs, psi(RFP)-tTF NPs, and psi-LF.

functional siRNA molecules in the cytosol. Before thiolation, TF showed a sharp peak of 12.0 ± 1.2 nm in the dynamic light-scattering measurement and appeared as small particles in TEM images (Figure 1B). After thiolation, tTF formed self-cross-linked NP structures in aqueous solution. The average hydrodynamic diameter of the tTF NPs was 124.2 ± 4.5 nm as measured by DLS, and the TEM images also demonstrated uniformly spherical tTF NPs, which were around 100 nm in size (Figure 1C).

To produce stable and compact psi-tTF NPs, poly siRNA (1 μg/1 μL HEPES buffer) was slowly added to the tTF (10 μg/1 μL PB buffer) and incubated for 24 h at 37 °C. In a gel-retardation assay, poly siRNA and 8.7 of amine-modified tTF built stable psi-tTF NPs at a weight ratio of 1:10 (Figure 1D). The initial particle-size distribution of the poly siRNA and tTF mixture showed a broad range of particle sizes from 10 nm to 1 μm, but NPs with a narrow size distribution were achieved at 24 h postincubation (Figure 1E). It was certified that monomeric and oligomeric tTF coexist under the buffer conditions, which means reversible inter- and intramolecular disulfide cross-linking between tTF monomer. However, a narrow size distribution of poly siRNA and tTF mixtures was achieved from 6 h postincubation, indicating that the self-conjugated tTF oligomers also react with poly siRNA to form stable psi-tTF NPs. On the basis of the observed PAGE gel and time-dependent changes in the particle size, the optimal mixing ratio of the poly siRNA and tTF was 1:10, and the optimum incubation time was 24 h. Under the optimized conditions, over 90% of the siRNA molecules were successfully encapsulated in the NPs and condensed by a chemical cross-linking reaction. The resulting psi-tTF NPs were compact, with a diameter of 343.2 ± 25.5 nm, which is larger than the diameter of natural TF and tTF self-assembled NPs (Figure 1F).


dx.doi.org/10.1021/bc400226b | Bioconjugate Chem. 2013, 24, 1850−1860

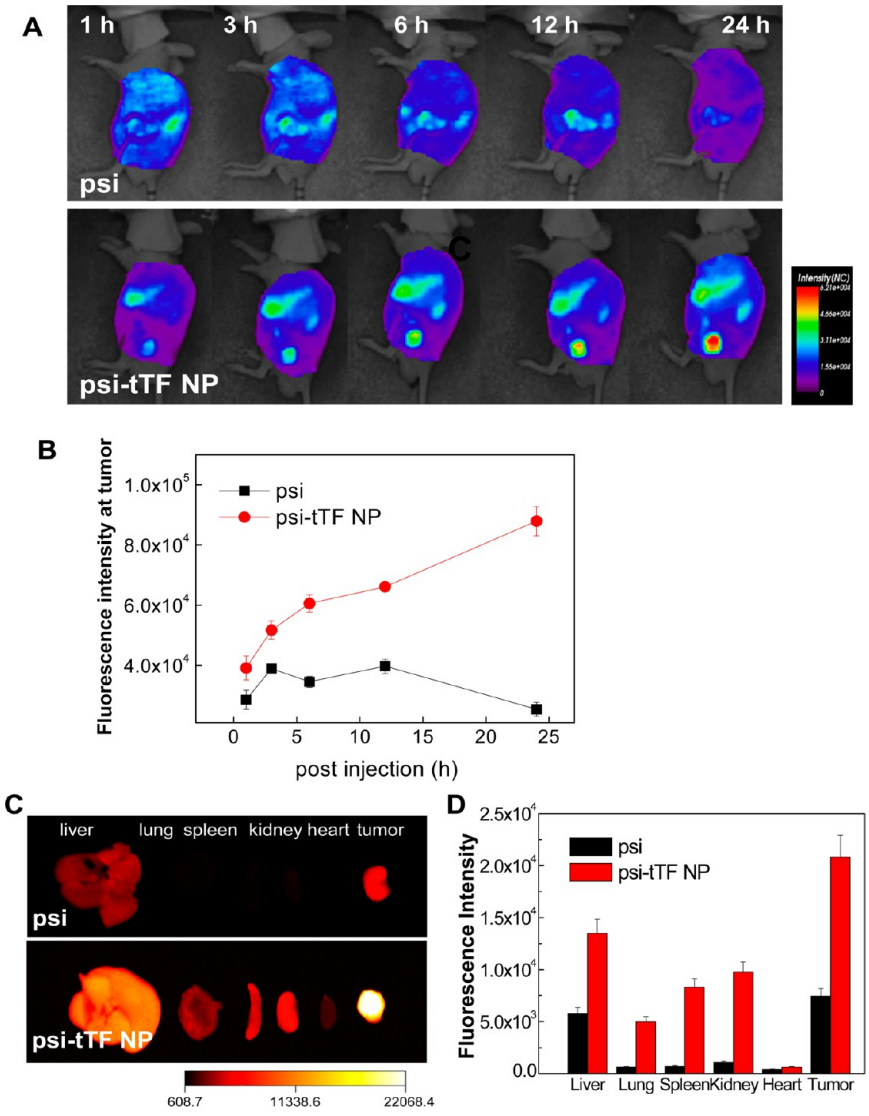


**Figure 6.** In vivo real-time and ex vivo NIRF imaging of psi-tTF-injected tumor-bearing mice. (A) Whole-body NIRF imaging of SCC-7 tumor-bearing mice after intravenous injection of psi (upper) and psi-tTF (lower). (B) Time-dependent NIRF intensity at the tumor site after the systemic injection of psi-tTF NPs. (C) Distribution of psi (upper) and psi-tTF (lower) in excised visceral organs and in the tumor. (D) Comparison of the NIRF intensity in excised tumors and visceral organs.

As a control, natural free siRNA did not have sufficient binding affinity to build nanostructures with both natural TF and tTF NPs. In the gel-retardation assay, large amounts of unbound mono siRNA molecules were observed in both mono-siRNA-TF and mono-siRNA-tTF incubated samples (Figure 2A). TEM images also confirmed that the mono siRNA did not form any particular structure with both natural TF and tTF (Figure 2B,C). The natural TF and the poly-siRNA mixture formed amorphous aggregates, with a partial disappearance of the band fraction of poly siRNA in the gel-retardation assay (Figure 2D). This might be due to the partial charge−charge interactions between them, resulting in loosely bound poly siRNA-TF conjugates, which were confirmed by TEM (Figure 2E).

In particular, the psi-tTF NPs produced were degradable and released mono siRNA under reductive conditions, and they protected the siRNA from enzymatic degradation. In general, animal cells have high levels of glutathione (5−10 mM) in their cytosol, and the cytosolic glutathione leads to a major destabilization of disulfide bonds.[26] In the gel-retardation assay, a large amount of mono siRNA was released from the particles after 10 mM DTT treatment (Figure 3A). In the TEM images, the DTT-treated psi-tTF NPs also showed a decrease in size and in electron density, with a loss of their spherical structure, pointing to the reversible degradation of the psi-tTF NPs in the reductive environment of the cytosol (Figure 3B). In addition, the psi-tTF NPs enhanced the RNase-resistant stability of the siRNA molecules in the blood. RNase-mediated siRNA degradation was gradually increased in both samples with increasing incubation time, but the siRNA formulated in the psi-tTF NPs was protected in the RNase-positive buffer for up to12 h (Figure 3C).

**Receptor-Mediated Cellular Uptake of the psi-tTF NPs.** The cellular uptake and intracellular distribution of the psi-tTF NPs were observed by fluorescence microscopy. The FPR-675-labeled poly siRNA (100 nM)-treated SCC-7 cells showed only marginal red fluorescence around the cell membrane, indicating extremely low cellular uptake of free siRNA. In contrast, the same dose of siRNA-formulated psi-tTF NPs-treated SCC-7 cells presented intense dual fluorescence


dx.doi.org/10.1021/bc400226b | Bioconjugate Chem. 2013, 24, 1850−1860

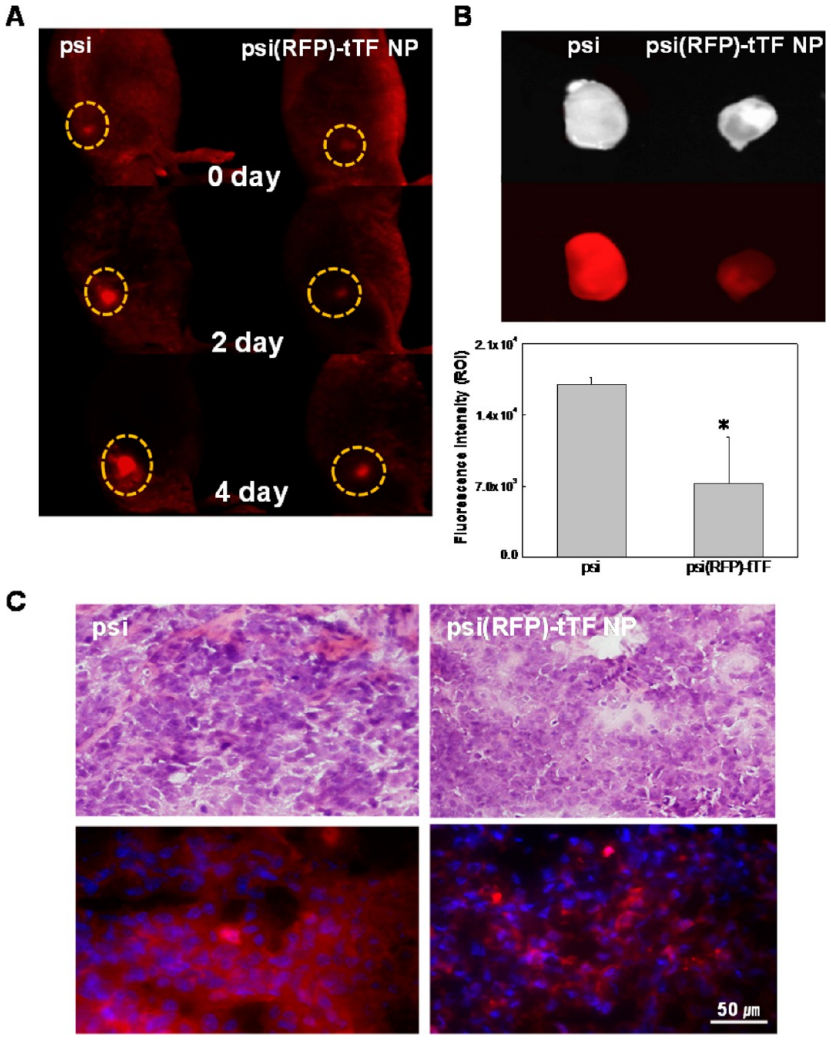


**Figure 7.** In vivo gene-silencing effects of the psi-tTF NPs in RFP/B16F10 tumor-bearing mice. (A) Time-dependent tumor RFP expression of paired psi and psi-tTF injected mice (yellow circle indicates the tumor site). (B) Ex vivo imaging of the excised tumors after 6 days (upper) and measured tumor RFP intensity (lower). The data represent the average ± SD from three mice. (C) Fluorescence images of the tumor tissues of paired mice 6 days postinjection. * $p < 0.05$ compared to the psi group.

that was excited by FITC-labeled tTF and FPR-675-labeled poly siRNA matched wavelengths (Figure 4A). This suggested that the psi-tTF NPs were internalized in the cytosol at the 30.8 μg/mL dose, which included 100 nM siRNA molecules. In a receptor competition-binding assay, the cellular uptake of the psi-tTF NPs was obviously reduced in the presence of free TF in the transfection medium. This was attributed mainly to the competitive binding of free TF to the TF receptors on the cancer cell membrane. The cellular uptake of the psi-tTF was also observed in B16F10 cells (Figure 4B). In the B16F10 cells, the psi-tTF NPs also showed enhanced cytoplasmic delivery of siRNA molecules. The cellular uptake of psi-tTF NPs in B16F10 cells was also reduced in TF-positive transfection media. On the basis of these results, we concluded that the enhanced delivery of siRNA by the psi-tTF NPs in vitro was closely associated with the transferrin receptor-mediated endocytosis pathway.

**In Vitro Cytotoxicity and Gene Silencing of the psi-tTF NPs.** To evaluate the cytotoxicity of the psi-tTF NPs, an MTT assay of RFP-expressing melanoma cancer cells (RFP/B16F10) was performed. As a positive control, poly siRNA formulated in a LF (psi-LF) was used to compare the cytotoxicity and the transfection efficiency. The psi-LF showed considerable toxicity in the MTT assay when the psi-LF concentration was >12.7 μg/mL (200 nM siRNA). The cell viability of the psi-LF-treated cells was 51.7 and 42.8% at siRNA concentrations of 200 and 400 nM, respectively. By contrast, the cell viability of the psi-tTF NPs was close to 96.8% at a concentration of 61.6 μg/mL (400 nM siRNA) (Figure 5A).

The in vitro gene-silencing efficacy was visualized at a concentration of 200 nM siRNA. Forty eight hours after transfection, the ratio of the RFP-expressing cells was 53.0% lower in the psi(RFP)-tTF NP-treated cells (Figure 5B). The number of RFP-expressing cells was also greatly decreased in the psi(RFP)-LF-treated cells, but the ratio of RFP-expressing cells was relatively high, resulting in severe cytotoxicity of the psi-LF cells (Figure 5C). The psi(sc)-tTF NPs-treated cells showed no significant difference in RFP expression compared to the control group, suggesting sequence-specific gene silencing of the delivered poly siRNA. In addition, the improved cell viability of the psi-tTF delivery system may be attributed to the biocompatibility of TF, which is an integral characteristic of natural materials.


dx.doi.org/10.1021/bc400226b | *Bioconjugate Chem.* 2013, 24, 1850−1860

**Biodistribution of the psi-tTF NPs in Tumor-Bearing Mice.** The psi-tTF NPs were prepared with FPR-675-labeled poly siRNA conjugates to evaluate the in vivo biodistribution of the psi-tTF NPs. The in vivo behavior of the naked poly siRNA and the psi-tTF NPs was noninvasively monitored by real-time NIRF imaging up to 24 h postinjection (Figure 6A). After the systemic injection of naked poly siRNA, the NIRF signal was markedly increased throughout the whole body followed by a rapid disappearance by renal clearance after 24 h. In contrast, the psi-tTF NP-injected mice showed intense fluorescence signals at the tumor site from 3 h postinjection. The fluorescence at the tumor site gradually increased, and the highest NIRF intensity in the tumor was observed at 24 h postinjection (Figure 6B). In particular, the tumor of the psi-tTF-injected mice was distinctly delineated from the surrounding normal tissues, suggesting that the psi-tTF NPs delivered the siRNA molecules more specifically to the tumor than to untargeted visceral organs. The ex vivo NIRF images from excised tissues also supported the accumulation of the psi-tTF NPs at the tumor site. In the psi-tTF-injected mice, the excised tumor showed higher NIRF signals than other visceral organs (Figure 6C). Compared to the naked poly siRNA-injected group, the psi-tTF NP-injected mice showed a 2.8-fold higher fluorescence intensity at the tumor site, suggesting tumor accumulation and an extended circulation time in the blood (Figure 6D). The longer blood circulation time and the active targeting property of the psi-tTF NPs contributed to the enhanced accumulation at the tumor.

**In Vivo Gene-Silencing Effect of the psi-tTF NPs.** The in vivo gene-silencing effect of the psi-tTF NPs was visualized by RFP gene knockdown in an RFP/B16F10-bearing mouse model. In real-time and noninvasive tumor fluorescence imaging, the psi-tTF NP-treated group showed significantly lower levels of RFP expression at tumors from 2 days post-treatment (Figure 7A). The difference in the RFP intensity was more distinct in the excised tumor. Compared to the naked poly siRNA-injected group, the fluorescence intensity at the tumor was decreased by 42.4%, on average, in the psi-tTF NP-injected group (Figure 7B). In the histological examination, tumor cells in the psi-tTF NP-injected mice showed significantly decreased RFP expression, which is in accordance with the results of the fluorescence imaging (Figure 7C).

To exclude nonspecific RFP downregulation, we compared tumor RFP of the psi(sc)-tTF NPs-treated mice with that of nontreated ones. The tumor RFP was not significantly reduced in the psi(sc)-tTF NPs-treated mice for 5 days (see Supporting Information, Figure S1). This indicated that the psi-tTF NPs could induce target-gene silencing by a sequence-specific mechanism.

## ■ DISCUSSION

The main objective of the present study was to develop a new biocompatible nanodelivery system for tumor-targeted delivery of siRNA by systemic administration. To achieve this goal, we considered TF, a natural macromolecule that is abundant in blood, as a siRNA carrier. TF is a serum protein that circulates for a longer time in the blood and shows more tumor-specific accumulation than other serum proteins.[27] The structure, function, and iron-binding properties as well as the potential of TF and its receptor in biomedical applications have been studied.[24,28,29] On the basis of findings from those studies, we fully expected that TF would have many advantages as a siRNA carrier for cancer specificity and biocompatibility.

Because natural TF rarely forms electrostatic conjugates with siRNA because of its low charge density, TF was chemically modified with functional thiol groups to enhance its interaction and chemical association with siRNA. In addition, we used structurally modified siRNA to enhance the binding affinity with tTF. As previously described, prudent structural modifications of siRNA can improve its physicochemical properties without a loss of gene-silencing activities.[19,21,26,30,31] Bioreducible poly siRNA with a 5′-end thiol modification has beneficial physicochemical properties, such as high molecular weight, high charge density, and functional thiol groups, enabling it to build stable and condensed nanostructures with cationic polymers.[19,21] A molecule of TF includes 58 lysine and 27 arginine residues (positively charged amino acids). In this study, the increased charge density of anionic poly siRNA might interact with partial positive residues of TF. Moreover, modified thiol groups in poly siRNA can contribute to the chemical cross-linking reaction of two molecules. It is well-known that most of thiol groups are converted into disulfide bonds within 24 h of incubation time[32] and that all thiols would be consumed after the whole conjugation process. Consequently, poly siRNA and tTF conjugates could interact to form stable and condensed NPs.

Characterization studies provided evidence for the formation of siRNA-carrying tTF NPs. More than 95% of RNA molecules were encapsulated in the NPs, and the psi-tTF NPs were degraded to release mono siRNA molecules under reductive conditions. After the cellular uptake, the psi-tTF NPs were expected to release monomeric siRNA by glutathione in the cytosol. The released siRNA molecules under cytosol-mimetic reductive conditions were confirmed by a gel-retardation assay, and the band fraction of the siRNA molecules was mainly distributed in 21 bp of monomeric form. The TEM images also showed changes in the psi-tTF NPs, suggesting disruption of the psi-tTF NPs. The released siRNA molecules were biologically active, and the target RFP was successfully downregulated in the RFP/B16F10 cells.

Because chemical modification may influence the affinity of TF for its receptor,[14] the binding affinity of the psi-tTF NPs for the TF receptor was examined. A receptor competition-binding assay verified that the cellular uptake of the psi-tTF NPs was critically dependent on the TF receptor-mediated endocytosis pathway. Although the cellular uptake of the psi-tTF NPs was not completely impeded by added free TF, it was markedly decreased for competitive binding of natural TF. This implies that the psi-tTF NPs retain considerable TF receptor-binding affinity and that they have receptor-binding residues on their surfaces. In common with other NPs that have a similar size distribution, the tumor-specific accumulation of the psi-tTF NPs might be primarily due to the effects of enhanced permeation and retention.[30,33,34] The psi-tTF NPs could provide additional advantages for receptor-specific, ligand-based targeting.

The in vivo tumor-targeted siRNA delivery of the psi-tTF NPs is attributed to their properties of tumor accumulation and efficient cellular uptake. Time-dependent whole-body NIRF imaging showed gradually increased NIRF at the tumor site of the psi-tTF NP-injected mice, suggesting that the psi-tTF NPs circulate for a long time in the blood. A longer blood circulation time allows the psi-tTF NPs to reach their therapeutic target and to accumulate in high numbers. Consequently, the psi-tTF NP-injected mice demonstrated significantly reduced tumor RFP throughout the experimental period. In addition to the

tumor specificity, the major benefit of using TF as a siRNA delivery vector is its biocompatibility. The psi-tTF showed very low toxicity at a transfection dose of 200 nM siRNA, whereas LF treatment resulted in severe toxicity, with the cell viability being under 50%. TF appeared to retain its biocompatibility even after thiolation and complexation with poly siRNA. Our study demonstrates the feasibility of using TF as a gene carrier. Although several challenges remain in relation to optimizing the preparation method for commercialization, the TF-based poly siRNA formulation could be a promising system for systemic siRNA delivery, particularly because of its prolonged circulation time in the blood and its high stability and biocompatibility.

## ■ CONCLUSIONS

We designed and synthesized a new nanosized siRNA carrier system utilizing TF and poly siRNA. Thiol-introduced TF was produced by modification of the primary amine of TF with a sulfhydryl group, and the resulting tTF spontaneously interacted with poly siRNA to form NPs. Our study revealed that psi-tTF NPs can protect siRNA from enzymatic degradation to transport siRNA molecules to tumor cells in a TF receptor-specific manner. After intravenous administration, the psi-tTF NPs accumulated in high numbers at the tumor region, presumably because of their prolonged circulation time in the blood and their tumor specificity. More importantly, the current study demonstrated effective target-gene silencing in vitro and in vivo without remarkable cytotoxicity. Considering their biocompatibility and tumor-homing properties, psi-tTF NPs could be a powerful candidate for a systemic siRNA delivery system for cancer therapy.

## ■ ASSOCIATED CONTENT

### Supporting Information

Time-dependent tumor RFP expression of paired nontreated and psi(sc)-tTF injected mice. This material is available free of charge via the Internet at http://pubs.acs.org.

## ■ AUTHOR INFORMATION


### Corresponding Authors

*Tel.: +82 2 958 6639; Fax: +82 2 958 5909; E-mail: sunkim@kist.re.kr (S.H.K.).

*Tel.: +82 2 958 5916; Fax: +82 2 958 5909; E-mail: kim@kist.re.kr (K.K.).

### Author Contributions

⊥These authors contributed equally to this work.


### Notes

The authors declare no competing financial interest.

## ■ ACKNOWLEDGMENTS

This study was funded by the GiRC Project (2012K1A1A2A01055811) and the Fusion Technology Project (NRF-2009-0081876) of MSIP, the M.D.−Ph.D. Program (2010-0019863, 2010-0019864) of MEST, and the Intramural Research Program (Young Fellow Program) of KIST.

## ■ REFERENCES


(1) Hammond, S. M., Boettcher, S., Caudy, A. A., Kobayashi, R., and Hannon, G. J. (2001) Argonaute2, a link between genetic and biochemical analyses of RNAi. *Science 293*, 1146−1150.

(2) Campbell, T. N., and Choy, F. Y. (2005) RNA interference: past, present and future. *Curr. Issues Mol. Biol. 7*, 1−6.

(3) Fire, A., Xu, S., Montgomery, M. K., Kostas, S. A., Driver, S. E., and Mello, C. C. (1998) Potent and specific genetic interference by double-stranded RNA in Caenorhabditis elegans. *Nature 391*, 806−811.

(4) Cheng, J. C., Moore, T. B., and Sakamoto, K. M. (2003) RNA interference and human disease. *Mol. Genet. Metab. 80*, 121−128.

(5) de Fougerolles, A. R. (2008) Delivery vehicles for small interfering RNA in vivo. *Hum. Gene Ther. 19*, 125−132.

(6) Gao, K., and Huang, L. (2009) Nonviral methods for siRNA delivery. *Mol. Pharmaceutics 6*, 651−658.

(7) Gebhart, C. L., and Kabanov, A. V. (2001) Evaluation of polyplexes as gene transfer agents. *J. Controlled Release 73*, 401−416.

(8) Hassani, Z., Lemkine, G. F., Erbacher, P., Palmier, K., Alfama, G., Giovannangeli, C., Behr, J. P., and Demeneix, B. A. (2005) Lipid-mediated siRNA delivery down-regulates exogenous gene expression in the mouse brain at picomolar levels. *J. Gene Med. 7*, 198−207.

(9) Zhang, S., Zhao, B., Jiang, H., Wang, B., and Ma, B. (2007) Cationic lipids and polymers mediated vectors for delivery of siRNA. *J. Controlled Release 123*, 1−10.

(10) Lv, H., Zhang, S., Wang, B., Cui, S., and Yan, J. (2006) Toxicity of cationic lipids and cationic polymers in gene delivery. *J. Controlled Release 114*, 100−109.

(11) Gatter, K. C., Brown, G., Trowbridge, I. S., Woolston, R. E., and Mason, D. Y. (1983) Transferrin receptors in human tissues: Their distribution and possible clinical relevance. *J. Clin. Pathol. 36*, 539−545.

(12) Citores, L., Ferreras, J. M., Munoz, R., Benitez, J., Jimenez, P., and Girbes, T. (2002) Targeting cancer cells with transferrin conjugates containing the non-toxic type 2 ribosome-inactivating proteins nigrin b or ebulin l. *Cancer Lett. 184*, 29−35.

(13) Dufes, C., Muller, J. M., Couet, W., Olivier, J. C., Uchegbu, I. F., and Schatzlein, A. G. (2004) Anticancer drug delivery with transferrin targeted polymeric chitosan vesicles. *Pharm. Res. 21*, 101−107.

(14) Zenke, M., Steinlein, P., Wagner, E., Cotten, M., Beug, H., and Birnstiel, M. L. (1990) Receptor-mediated endocytosis of transferrin-polycation conjugates: An efficient way to introduce DNA into hematopoietic cells. *Proc. Natl. Acad. Sci. U.S.A. 87*, 3655−3659.

(15) Liang, K. W., Hoffman, E. P., and Huang, L. (2000) Targeted delivery of plasmid DNA to myogenic cells via transferrin-conjugated peptide nucleic acid. *Mol. Ther. 1*, 236−243.

(16) Choi, C. H., Alabi, C. A., Webster, P., and Davis, M. E. (2010) Mechanism of active targeting in solid tumors with transferrin-containing gold nanoparticles. *Proc. Natl. Acad. Sci. U.S.A 107*, 1235−1240.

(17) Dubljevic, V., Sali, A., and Goding, J. W. (1999) A conserved RGD (Arg-Gly-Asp) motif in the transferrin receptor is required for binding to transferrin. *Biochem. J. 341*, 11−14.

(18) van Agthoven, A., Goridis, C., Naquet, P., Pierres, A., and Pierres, M. (1984) Structural characteristics of the mouse transferrin receptor. *Eur. J. Biochem. 140*, 433−440.

(19) Lee, S. J., Huh, M. S., Lee, S. Y., Min, S., Lee, S., Koo, H., Chu, J. U., Lee, K. E., Jeon, H., Choi, Y., Choi, K., Byun, Y., Jeong, S. Y., Park, K., Kim, K., and Kwon, I. C. (2012) Tumor-homing poly-siRNA/glycol chitosan self-cross-linked nanoparticles for systemic siRNA delivery in cancer treatment. *Angew. Chem., Int. Ed. 51*, 7203−7207.

(20) Huh, M. S., Lee, S. Y., Park, S., Lee, S., Chung, H., Choi, Y., Oh, Y. K., Park, J. H., Jeong, S. Y., Choi, K., Kim, K., and Kwon, I. C. (2010) Tumor-homing glycol chitosan/polyethylenimine nanoparticles for the systemic delivery of siRNA in tumor-bearing mice. *J. Controlled Release 144*, 134−143.

(21) Lee, S. Y., Huh, M. S., Lee, S., Lee, S. J., Chung, H., Park, J. H., Oh, Y. K., Choi, K., Kim, K., and Kwon, I. C. (2010) Stability and cellular uptake of polymerized siRNA (poly-siRNA)/polyethylenimine (PEI) complexes for efficient gene silencing. *J. Controlled Release 141*, 339−346.

(22) Kratz, F., Beyer, U., Roth, T., Tarasova, N., Collery, P., Lechenault, F., Cazabat, A., Schumacher, P., Unger, C., and Falken, U. (1998) Transferrin conjugates of doxorubicin: Synthesis, character-

ization, cellular uptake, and in vitro efficacy. *J. Pharm. Sci. 87*, 338−346.
(23) Kearsley, J. H., Furlong, K. L., Cooke, R. A., and Waters, M. J. (1990) An immunohistochemical assessment of cellular proliferation markers in head and neck squamous cell cancers. *Br. J. Cancer 61*, 821−827.
(24) Qian, Z. M., Li, H., Sun, H., and Ho, K. (2002) Targeted drug delivery via the transferrin receptor-mediated endocytosis pathway. *Pharmacol. Rev. 54*, 561−587.
(25) Vijaykumar, V., and Topp, E. M. (1995) Diffusion of an anti-transferrin receptor antibody in cultured murine melanoma cell layers. *Pharm. Res. 12*, 1907−1916.
(26) Mok, H., Lee, S. H., Park, J. W., and Park, T. G. (2010) Multimeric small interfering ribonucleic acid for highly efficient sequence-specific gene silencing. *Nat. Mater. 9*, 272−278.
(27) Becker, A., Riefke, B., Ebert, B., Sukowski, U., Rinneberg, H., Semmler, W., and Licha, K. (2000) Macromolecular contrast agents for optical imaging of tumors: Comparison of indotricarbocyanine-labeled human serum albumin and transferrin. *Photochem. Photobiol. 72*, 234−241.
(28) Richardson, D. R., and Ponka, P. (1997) The molecular mechanisms of the metabolism and transport of iron in normal and neoplastic cells. *Biochim. Biophys. Acta 1331*, 1−40.
(29) Lieu, P. T., Heiskala, M., Peterson, P. A., and Yang, Y. (2001) The roles of iron in health and disease. *Mol. Aspects Med. 22*, 1−87.
(30) Lee, S. J., Son, S., Yhee, J. Y., Choi, K., Kwon, I. C., Kim, S. H., and Kim, K. (2013) Structural modification of siRNA for efficient gene silencing. *Biotechnol. Adv. 31*, 491−503.
(31) Bolcato-Bellemin, A. L., Bonnet, M. E., Creusat, G., Erbacher, P., and Behr, J. P. (2007) Sticky overhangs enhance siRNA-mediated gene silencing. *Proc. Natl. Acad. Sci. U.S.A. 104*, 16050−16055.
(32) Son, S., Singha, K., and Kim, W. J. (2010) Bioreducible BPEI-SS-PEG-cNGR polymer as a tumor targeted nonviral gene carrier. *Biomaterials 31*, 6344−6354.
(33) Matsumura, Y., and Maeda, H. (1986) A new concept for macromolecular therapeutics in cancer chemotherapy: mechanism of tumoritropic accumulation of proteins and the antitumor agent smancs. *Cancer Res. 46*, 6387−6392.
(34) Kim, J. H., Kim, Y. S., Park, K., Kang, E., Lee, S., Nam, H. Y., Kim, K., Park, J. H., Chi, D. Y., Park, R. W., Kim, I. S., Choi, K., and Chan Kwon, I. (2008) Self-assembled glycol chitosan nanoparticles for the sustained and prolonged delivery of antiangiogenic small peptide drugs in cancer therapy. *Biomaterials 29*, 1920−1930.